Stimulated Raman adiabatic passage with partially coherent laser fields

L. P. Yatsenko and V. I. Romanenko*
Institute of Physics, Ukrainian Acadaemy of Sciences, Prospect Nauki 46, Kiev-39, 03650, Ukraine

B. W. Shore and K. Bergmann
Universität Kaiserslautern, 67653 Kaiserslautern, Germany
(Received 16 October 2001; published 4 April 2002)

In this paper we discuss the effect of phase noise upon the efficiency of population transfer produced by stimulated Raman adiabatic passage (STIRAP). To allow an adjustable cross-correlation of the two fields we consider the pump and Stokes pulses to be derived from a single phase-diffusing exponentially correlated laser, but we allow some time delay T between the noise signals. We present examples of Monte Carlo simulations, showing unexpected regularities in the dependence of efficiency upon pulse area for partially cross-correlated fields: efficiency does not monotonically increase with increasing pulse area, as would be expected. We explain these, and other properties, by using a simple model of pulse shapes to derive analytic expressions for efficiency. Although derived for a specific analytic form, the formulas also provide a useful description of transfer efficiency by other pulse shapes. We also obtain an estimate of the fundamental limit on the transfer efficiency with STIRAP, based on the Schawlow-Townes limit to laser bandwidths.

DOI: 10.1103/PhysRevA.65.043409 PACS number(s): 32.80.Bx, 42.50.Gy, 42.50.Hz

I. INTRODUCTION

Stimulated Raman adiabatic passage (STIRAP) has been intensively investigated for more than 15 years (see [1] and references therein) as a technique for transferring population between selected quantum states. In the most elementary applications of this technique a three-state atom is exposed to two sequential partially overlapping laser pulses. Initially the population resides in state 1, and the intended target of the population, state 3, is entirely unpopulated. An excited state, state 2, has energy above both of these states and serves as an intermediary for the population transfer, though it has negligible population at all times. (Depicted on an energy scale, the linkage pattern of the radiative interaction of such a Raman process has the appearance of a lambda.) The first pulse has a carrier frequency close to the Bohr transition frequency between states 3 and 2, whereas the carrier frequency of the later pulse is close to the Bohr frequency of the transition between states 1 and 2. Although neither of these pulses needs to fulfil a single-photon resonance condition, it is necessary that the two pulses fulfill a two-photon resonance condition: the difference between the two carrier frequencies must equal the difference between the two Bohr frequencies. If the pulse envelopes are smooth and the pulse fluences are sufficiently large (more precisely, the time integral of the Rabi frequencies—the pulse areas—must be sufficiently large for each pulse), then the population transfer can be very nearly complete.

To ensure maximum population transfer it is important to understand, and then control, the various factors that prevent ideal operation of the STIRAP process in practice. One of the most important factors is the deviation of actual laser pulses from the mathematical ideal of a smooth envelope over an otherwise monochromatic carrier wave—the so-called bandwidth-limited pulse. Deviations may occur for many reasons, some of which require extra care to ensure that all of the laser components remain isolated from vibrations and other environmental irregularities. Ultimately one is led to consider the intrinsic bandwidth of the laser, usually regarded as originating in random variations in the laser phase or, because the time derivative of the phase is the instantaneous frequency, in uncontrollable variations in the laser frequency, usually expressed as the detuning from resonance.

The key to successful population transfer with STIRAP is the association of the state vector $\Psi(t)$ with one of three independent time-dependent adiabatic states, the so-called population trapping state or dark state $\Phi_d(t)$, and the maintenance of that identification during the pulse sequence (in which the Stokes pulse precedes but overlaps the pump pulse). It is essential for this purpose that a two-photon resonance condition be maintained. To the extent that there is nonadiabatic evolution, or there is nonzero two-photon detuning, then the state vector $\Psi(t)$ will deviate from the dark state $\Phi_d(t)$ and population transfer will be incomplete.

II. HISTORICAL CONTEXT

There has been much work, both theoretical and experimental, elucidating the conditions needed for complete population transfer within the STIRAP procedure and for maintaining the statevector as the dark state. We here note some of these to make clear the differences with what we present here.

A. Static detuning

The dependence of population-transfer efficiency upon two-photon detuning (sometimes referred to as an evaluation of the two-photon linewidth) in the absence of noise has been examined by Romanenko and Yatsenko [2]. This two-photon linewidth is connected with the mixing of the excited

*Electronic address: vr@iop.kiev.ua

state into the adiabatic state when the two-photon resonance is not maintained [[2], formula (19)].

Such efficiency is closely tied to the requirement that the time evolution be adiabatic, as expressed by the requirement that the rate of change in a mixing angle $\theta(t)$ be small (see below). Prior studies of STIRAP dealt primarily with smooth noiseless pulse amplitudes, such as Gaussian pulses, when estimating two-photon linewidths. Here we supplement those earlier studies by introducing explicitly noisy pulses.

B. Noise

It is important to realize that, although it is convenient to characterize the noise properties of a laser by a single number, the laser bandwidth, this simplification may be inadequate for predicting effects produced by the laser: a variety of phase and amplitude variations can produce the same bandwidth, yet have very different effects upon excitation, fluorescence and other laser-induced processes [3,4]. We offer further comments below.

Some years ago, when the interesting properties of population trapping in the steady-excitation lambda system were first studied [5–9] a number of investigations examined the effect of finite laser bandwidth upon the maintenance of the trapped state. In these early works there was no concern with pulse sequences, only with steady illumination by noisy lasers.

1. The WL process

Much of that work was based upon modeling the laser noise with the phase-diffusion model suggested by Glauber [10]. In this model the fluctuating part of the derivative of the laser phase (an instantaneous frequency offset) is regarded as a stochastic variable $\xi(t)$. Specifically $\xi(t)$ is taken to be a zero-mean Gaussian Markov process. In this Wiener-Levy (WL) process [11] the two stochastic variables are fully defined by the properties

$$\langle \xi_j(t)\rangle = 0, \quad \langle \xi_j(t)\xi_k(t')\rangle = 2D_{jk}\delta(t-t'), \tag{2.1}$$

where $\delta(x)$ is the Dirac delta and the brackets $\langle\cdots\rangle$ denote an ensemble average. Such δ-function-correlated white noise is associated with a Lorentzian profile of the intensity distribution (D_{jj} is the bandwith of laser j and D_{PS} is the cross correlation of the two lasers). The Lorentzian profile is not a good description of the wings of any laser spectrum, but it is acceptable for describing small detunings. It characterizes the noise by a single parameter, the laser bandwidth. This phase-diffusion model of laser noise was used in the description of single-laser excitation of atoms or molecules [12–16].

The great theoretical utility of the WL stochastic model is that, as Agarwal showed [14], when it is used with Liouville (density matrix) equations of time evolution, then the stochastic variables in these equations can be replaced by constant relaxation coefficients D_{mn} that parametrize the laser bandwidth and cross correlation.

The first attempt to apply this model to the treatment of population trapping were by Dalton and Knight [8,9]. They showed that when there was no cross correlation, then phase fluctuations of the two independent lasers (i.e., finite laser bandwidths) caused the population trapping to fail, but that when the two lasers were well cross correlated, then the noise canceled, so that two-photon coherences were unaffected and population trapping was preserved.

Although qualitative and quantitative analyses of the effect of phase-diffusion noise (white noise) on the lambda (and ladder) system have been published (e.g., [17]), the presence of counterintuitive pulse sequences, such as the one that occurs with STIRAP, present additional aspects of population trapping that have not been addressed.

Successful population transfer with STIRAP requires maintenance of the adiabatic trapped state, and in this respect there is commonality with studies of fluorescence. But with STIRAP there can be other causes of failed population transfer in addition to phase fluctuations.

2. The OU Process

Already in the early papers on STIRAP there was concern about the effect of laser bandwidth upon the success of the population transfer, and Kuhn *et al.* [17] carried out numerical simulation of a noisy laser. They used a stochastic model of zero-mean exponentially correlated noise (an *Ornstein-Uhlenbeck* or OU process), but they assumed null cross correlation

$$\langle \xi_j(t)\rangle = 0, \ \langle \xi_j(t)\xi_k(t')\rangle = \begin{cases} D_j G_j \exp(-G_j|t-t'|), & j=k \\ 0, & j\neq k. \end{cases} \tag{2.2}$$

Here D is the spectral density of the noise and G is its bandwidth (G^{-1} is the correlation time of the fluctuations). The OU model was used for treatment of laser excitation by a number of authors [18–20].

For large values of $G \gg D$, $\xi(t)$ is a δ-function-correlated process

$$\langle \xi(t)\xi(t')\rangle = 2D\delta(t-t'). \tag{2.3}$$

In this case, D is the phase-diffusion coefficient and the spectrum of the intensity has a Lorenzian profile; as noted above, D is the intensity half-width at half maximum (HWHM).

The opposite case, $G \ll D$, is close to the extreme case of an ensemble of fields with constant frequencies that obey Gaussian statistics with variance DG. The intensity profile is then a Gaussian; the HWHM is $\sqrt{2\ln 2}\sqrt{DG}$.

Because the OU process incorporates two parameters D and G, the laser bandwidth alone is not sufficient to define the process fully. Predictions based on the OU process can be more realistic, but they require more complete characterization of the laser noise than bandwidth.

3. Other processes

A variety of other forms of noise have been used in treatments of steady single-laser excitation. These include various forms of random-telegraph noise and pre-Gaussian noise, as well as random fluctuations in amplitude (see [3,4,21]). These models have not as yet been used with multifrequency pulsed excitation.

C. Numerical implementation

Two approaches to the treatment of noise have generally been followed. In one approach, set forth by Agarwal and followed by others, the definitions of the stochastic processes are used to derive equations of motion for the density matrix. In these equations all effects of noise appear as relaxation rates, much as do the parameters T_1 and T_2 in the Bloch equations for a two-state atom. This approach permits the inclusion of cross correlation between two laser beams; the degree of independence is an adjustable parameter. This is the approach used by Dalton and Knight [8,9].

In the other approach, one carries out Monte Carlo simulation, averaging over many realizations of time histories of the noise. In the work of Kuhn *et al.* [17] and also the present work, the procedure of Fox *et al.* [22] is used to create a sequence of values for the stochastic variables $\xi_j(t)$ at a sequence of discrete times [22,23]. We implement a variant of this technique, as noted below.

In the Kuhn work, the Stokes and pump fields were taken as independent processes. These extensive simulations [17] gave quantitative indications of the detrimental effects of phase fluctuations when the pulses were shorter than the intermediate-state radiative lifetime. From that work came a simple phenomonological formula, consistent with experimental evidence, for use in estimating how a fluctuation bandwidth can quantitatively affect the completeness of population transfer. The contrasting regime, of pulse durations longer than the radiative lifetime, remained still to be investigated.

D. Present work

It is most important, for the success of the STIRAP procedure, that the two-photon resonance condition be fulfilled. For some time it has been recognized [8,9] that when the two laser pulses are derived from a single laser source, then beneficial cancellations of phase fluctuations may occur, so that population transfer is more successful than it would be if the two lasers were entirely independent.

In this paper we examine this situation in more detail. We allow variable cross correlation by assuming that the two fields are both derived from a common source (i.e., they have the same fluctuations) but they are offset in time by a delay T. The parameter T provides a measure of cross correlation. The behavior of such a model system is expected to give a good description of the ultimate intrinsic limits on maximum population transfer possible with the STIRAP technique.

Using this simple model for the laser phase fluctuations we show that the population transfer efficiency (i.e., the fraction of the total population that is found in the target state after the pulse sequence concludes) shows some remarkable and unexpected regularities. These regularities, quite visible in Monte Carlo simulations, have a simple explanation, as we demonstrate by means of analytic approximations.

To achieve our analytic results we assume a very special form for the two pulses, but we demonstrate with numerical simulation that the regularities occur with other pulse shapes, for which analytic results are not available.

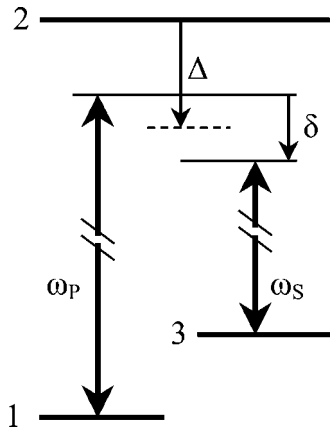

FIG. 1. Schematic diagram of energy levels 1, 2, 3, carrier frequencies ω_S and ω_P, and detunings δ and Δ.

The frequency fluctuations of common single-frequency cw lasers are caused by low-frequency fluctuations in the environment (e.g., mechanical vibrations of the laser mountings). For these the OU model with $G \ll D$ can be a good approximation. We therefore adopt the OU process, Eq. (2.2), as a model of phase noise.

III. BASIC EQUATIONS

We consider a three-state atom with excitation linkages in the usual lambda form: two long-lived low-energy states ψ_1 and ψ_3, each linked via electric-dipole interaction to an excited state ψ_2. Figure 1 shows the energy level structure and defines the various carrier frequencies (ω_S, ω_P) and detunings (δ, Δ) used subsequently. We assume that the spontaneous radiative decay of the excited state, which occurs at rate γ, goes entirely to states other than ψ_1 and ψ_3, and that there are no interactions linking ψ_1 and ψ_3 directly. The atom interacts, via dipole transition moments **d**, with the electric field $\mathbf{E}(t)$ of two pulses, termed Stokes (S) and pump (P),

$$\mathbf{E}(t) = \mathbf{E}_P(t)\cos(\omega_P t + \varphi_P) + \mathbf{E}_S(t)\cos(\omega_S t + \varphi_S). \tag{3.1}$$

These have carrier frequencies ω_P and ω_S that are close to the $1 \leftrightarrow 2$ and $2 \leftrightarrow 3$ Bohr transition frequencies, respectively. The phases of the fields, φ_P and φ_S, we take to be stochastic functions of time (noise sources); their time derivatives are the stochastic functions $\xi_j(t)$

$$\dot{\varphi}_j(t) = \xi_j(t), \quad j = \{S, P\}. \tag{3.2}$$

The pulse amplitudes $|\mathbf{E}_P(t)|$ and $|\mathbf{E}_S(t)|$ are smooth, nonfluctuating functions of time, with the Stokes pulse arriving first.

As a first (standard) step, we express the statevector $\Psi(t)$ in terms of the basic physical (''bare'') states $\tilde{\psi}_j$ through the expansion

$$\Psi(t) = \sum_j C_j(t)\exp[-i\zeta_j(t)]\tilde{\psi}_j \equiv \sum_j C_j(t)\psi_j(t),$$

$$j=\{1,2,3\}, \tag{3.3}$$

where the phases $\zeta_j(t)$, to be specified below, define a "rotating" reference frame of basis states $\psi_j(t)=\exp[-i\zeta_j(t)]\tilde{\psi}_j$ for the probability amplitudes $C_j(t)$. We take the atom to be initially in the state ψ_1.

From the time-dependent Schrödinger equation we obtain the coupled equations

$$\frac{d}{dt}\mathbf{C}(t)=-i\mathsf{W}(t)\mathbf{C}(t), \tag{3.4}$$

where $\mathbf{C}(t)$ is a three-component column vector, with elements $\{C_1(t),C_2(t),C_3(t)\}$, and $\mathsf{W}(t)$ is a 3×3 matrix, a representation of the Hamiltonian in the time-varying basis. As is customary (cf. [24]), we treat the radiative interaction within the rotating-wave approximation (RWA), meaning that we choose the phases to eliminate rapidly varying exponentials, equivalent to the conditions

$$\dot{\zeta}_1=\dot{\zeta}_2-\omega_P-\xi_P, \quad \dot{\zeta}_3=\dot{\zeta}_2-\omega_S-\xi_S, \tag{3.5}$$

and neglect counterrotating terms. The resulting RWA Hamiltonian matrix reads

$$\mathsf{W}^{(RWA)}(t)=\frac{1}{2}\begin{bmatrix} -\delta+2\xi_P & \Omega_P(t) & 0 \\ \Omega_P(t) & -2\Delta-i\gamma & \Omega_S(t) \\ 0 & \Omega_S(t) & +\delta+2\xi_S \end{bmatrix}. \tag{3.6}$$

Here the off-diagonal elements

$$\Omega_P(t)=-\langle 1|\mathbf{d}\cdot\mathbf{E}_P(t)|2\rangle, \quad \Omega_S(t)=-\langle 3|\mathbf{d}\cdot\mathbf{E}_S(t)|2\rangle \tag{3.7}$$

are slowly varying real-valued functions of time, and the diagonal elements are expressed in terms of the average single-photon detuning Δ and the two-photon detuning δ (see Fig. 1),

$$\hbar\delta\equiv\hbar(\omega_S-\omega_P)-E_1+E_3, \tag{3.8}$$

$$\hbar\Delta\equiv\frac{\hbar}{2}(\omega_P+\omega_S)+\frac{1}{2}(E_1+E_3)-E_2. \tag{3.9}$$

As in earlier work (see Ref. [25]), it is convenient for further analysis to express the RWA Hamiltonian matrix in an alternative basis, using the time-dependent "bright" state $\Phi_b(t)$ and "dark" state $\Phi_d(t)$,

$$\begin{bmatrix} \Phi_b(t) \\ \Phi_2(t) \\ \Phi_d(t) \end{bmatrix}=\begin{bmatrix} \sin\theta(t) & 0 & \cos\theta(t) \\ 0 & 1 & 0 \\ \cos\theta(t) & 0 & -\sin\theta(t) \end{bmatrix}\begin{bmatrix} \psi_1(t) \\ \psi_2(t) \\ \psi_3(t) \end{bmatrix}. \tag{3.10}$$

These definitions involve the time-dependent mixing angle $\theta(t)$

$$\tan\theta(t)=\Omega_P(t)/\Omega_S(t). \tag{3.11}$$

The expansion of the statevector in this basis reads

$$\Psi(t)=C_b(t)\Phi_b(t)+C_2(t)\Phi_2(t)+C_d(t)\Phi_d(t). \tag{3.12}$$

From the time-dependent Schrödinger equation we obtain the coupled equations of the form (3.4) with the amplitudes $\{C_b(t),C_2(t),C_d(t)\}$ forming the elements of the column vector $\mathbf{C}(t)$.

With our assumed pulse sequence, of Stokes before pump, the dark state $\Phi_d(t)$ coincides initially with the initially populated bare state ψ_1, and it aligns after the pulse sequence with the target state ψ_3. Thus by maintaining the statevector $\Psi(t)$ in this dark state at all times, we accomplish the population transfer $\psi_1\rightarrow\psi_3$ of a traditional STIRAP process.

For the population transfer to be complete, the mixing angle $\theta(t)$ must slowly change from 0 to $\pi/2$ and, in the absence of phase fluctuations, $\xi_P=0$ and $\xi_S=0$, the two-photon resonance condition ($\delta=0$) must be maintained. Under these conditions neither of the states $\Phi_b(t)$ or $\Phi_2(t)$ become populated.

In this bright-dark basis, with the component ordering $\{b,2,d\}$, the RWA Hamiltonian matrix reads (with suppression of explicit notation of time dependence) as

$$\mathsf{W}^{(BD)}=\frac{1}{2}\begin{bmatrix} 2\xi_S\cos^2\theta+2\xi_P\sin^2\theta+\delta\cos2\theta & \Omega_{rms} & +2i\dot{\theta}-(\xi_S-\xi_P+\delta)\sin2\theta \\ \Omega_{rms} & -2\Delta-i\gamma & 0 \\ -2i\dot{\theta}-(\xi_S-\xi_P+\delta)\sin2\theta & 0 & 2\xi_S\sin^2\theta+2\xi_P\cos^2\theta-\delta\cos2\theta \end{bmatrix}. \tag{3.13}$$

Here the rms Rabi frequency $\Omega_{rms}(t)$ is

$$\Omega_{rms}(t)=\sqrt{\Omega_P(t)^2+\Omega_S(t)^2}. \tag{3.14}$$

The transformed Hamiltonian matrix includes, in addition to the usual nonadiabatic coupling introduced as the time derivative of the mixing angle $\dot{\theta}$, some time derivatives of the Stokes and pump phases. To maintain the statevector as the dark state, the matrix elements in the upper right and lower left corners must be negligible. This requires, in addition to the usual need for small $\dot{\theta}$, a small value for the instanta-

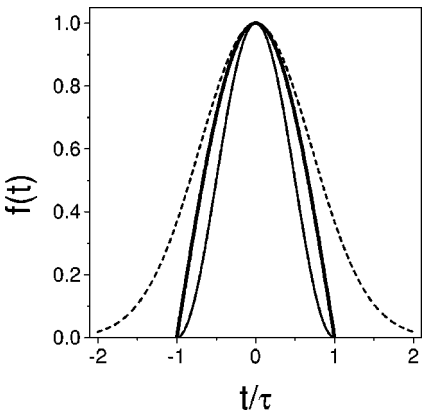

FIG. 2. Pulse shape $f(t)$ for the three forms used in this work: thick line is cos, Eq. (3.16); the thin line is $\cos^2$, Eq. (3.17); and the dashed line is Gaussian, Eq. (3.18).

neous frequency difference $\xi_S-\xi_P$. We immediately recognize the importance of possible correlation of the two-phase fluctuations: if the time derivatives of the phases are the same then their fluctuations cancel and the dynamics is that of conventional STIRAP.

A. Pulse shapes

In the present work we took the Stokes and pump amplitudes to be of equal magnitude and shape, but offset in time by t_d,

$$\Omega_S(t)=\Omega_0 f(t), \quad \Omega_P(t)=\Omega_0 f(t-t_d). \tag{3.15}$$

For the pulse-shape function $f(t)$ we used several analytic expressions: a cos pulse

$$f(t)=\begin{cases}\cos\left[\dfrac{\pi}{2}\dfrac{t}{\tau}\right], & -\tau<t<\tau,\\ 0 \quad \text{otherwise},\end{cases} \tag{3.16}$$

useful for analytical evaluation of various integrals; a $\cos^2$ pulse

$$f(t)=\begin{cases}\cos^2\left[\dfrac{\pi}{2}\dfrac{t}{\tau}\right], & -\tau<t<\tau,\\ 0 \quad \text{otherwise},\end{cases} \tag{3.17}$$

useful as a second example of a finite-duration pulse for simulations; and a Gaussian pulse

$$f(t)=\exp[-(t/\tau)^2]. \tag{3.18}$$

In our numerical simulation the latter are used only within a finite time window. Figure 2 shows the three shapes. For cos pulses (3.16) we consider only the delay $t_d=\tau$. For the other pulses the time delay is adjustable, and was chosen to produce the most effective population transfer: $t_d=0.6\tau$ for $\cos^2$ and $t_d=0.9\tau$ for Gaussian.

B. Noise model

Numerical simulation of phase fluctuations can be carried out by averaging a succession of time histories, for each of which the frequency $\xi(t)$ is a realization of exponentially correlated colored noise (an example of Monte Carlo simulation). Such functions can be generated using the algorithm described by Fox and others [22,23], as was done in Ref. [17]. In brief, we obtain a sequence of values $\xi(t_j)$ at discrete times $t_j=t_{j-1}+\Delta t$ separated by the step Δt. The value of $\xi(t_{j+1})$ emerges from $\xi(t_j)$ according to the algorithm

$$\xi(t_{j+1})=\xi(t_j)\exp(-G\Delta t)+h(t_j), \tag{3.19}$$

where the sequence of values $h(t_j)$ obey Gaussian statistics with a zero first moment and the second moment given by

$$\langle h^2(t_j)\rangle = DG(1-e^{-2G\Delta t}). \tag{3.20}$$

We formed the sequence of $\xi(t_j)$ with the variance DG using the standard Matlab function *randn.*

To model the effect of variable cross correlation we assume that the pump and Stokes fields follow the same statistics, but that they may be offset in time by T. Specifically, we assume

$$\xi_S(t)=\xi_P(t+T). \tag{3.21}$$

The delay T provides an additional parameter, beyond D and G, with which to characterize the radiation. For $T=0$ the two fields are perfectly correlated, and the two-photon detuning is zero at all times. For very large T (compared with the duration of the atom-field interaction and the correlation time of the noise) the fluctuations become independent, as was assumed in an earlier work [17].

Both positive and negative values of the time delay T are possible. In the STIRAP process with two pulses generated by the single laser one can expect $T=t_d$, where t_d is the time delay between pulses. If the STIRAP process is carried out in an atomic or molecular beam crossing two spatially displaced laser beams then any value and sign of T can be realized by adjusting the optical paths of pump and Stokes beams.

IV. SIMULATION RESULTS

This section presents numerical results, obtained by Monte Carlo simulation of the Schrödinger equation, for pulses of the form (3.16), (3.17), and (3.18). We compare these simulations with the theory developed in Sec. V. In summary, our model of excitation involves the following parameters, in addition to one-photon detuning Δ and two-photon detuning δ: Ω_0 is the peak Rabi frequency, γ is the spontaneous emission rate of state 2; G is the inverse autocorrelation time for the noise ($G\gg D$ implies white noise); D is the phase diffusion coefficient (the amplitude of white-noise fluctuations); T is the delay between the two noise sources that generate the random phases of the fields ($T\rightarrow\infty$ implies no cross-correlation).

We use these frequencies X in the dimensionless product form $X\tau$ where appropriate.

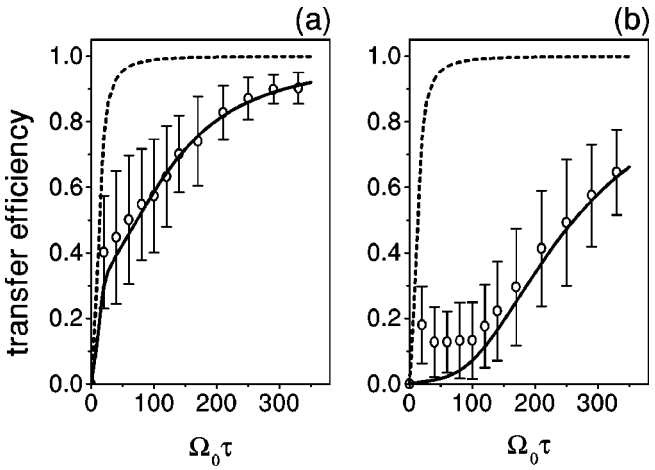

FIG. 3. Population transfer efficiency versus pulse area $\Omega_0\tau$, with $\delta=0$, $\Delta=0$, for cos pulses, shape (3.16), when fields are independent, $T=2\tau$. Circles depict Monte Carlo simulation, solid lines show theory, and dashed lines depict the transfer efficiency without noise. Bars show the root mean square of the deviation of population transfer efficiency from the average transfer efficiency. Parameters are $\gamma\tau=10$, $G\tau=50$. Frame (a) $D\tau=2$; frame (b) $D\tau=10$.

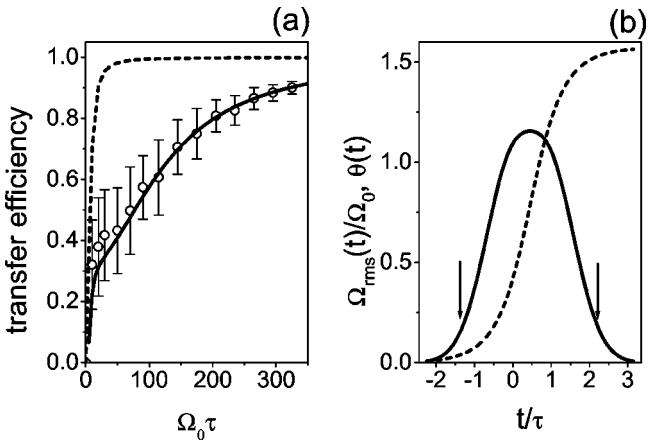

FIG. 4. (a) Population transfer efficiency versus pulse area $\Omega_0\tau$, with $\delta=0$, $\Delta=0$, for Gaussian pulses, shape (3.18), when fields are independent, $T=20\tau$. Parameters are $\gamma\tau=10$, $G\tau=50$, $D\tau=1$, $t_d=0.9\tau$. Points and lines are as in Fig. 3. (b) The thick line is the root mean square of the two pulses Ω_{rms} versus time. Arrows show bounds of the time-integration window. The dashed line is θ versus time.

A. Uncorrelated fields (large $|T|$)

Figure 3 presents examples of population transfer efficiency versus pulse area (parameterized by the product of peak Rabi frequency Ω_0 and pulse duration τ), when the phase fluctuations of the two pulses are independent. (The computations used $T=2\tau$. We have found that this is sufficient to give results that are unchanged for larger T.)

The dashed line shows the dependence of transfer efficiency on pulse area in the absence of any noise. This dashed curve shows a well-known behavior: as pulse areas increase the time evolution becomes more adiabatic and the population transfer becomes more complete. For the example shown here, a pulse area exceeding 10^2 is needed for good efficiency when there is no noise.

The circles mark the results obtained by Monte Carlo simulation. Each point is the average of 100 realizations of the stochastic process. To indicate the width of the statistical distribution of transfer efficiency the bars show the root mean square of the deviation of population transfer efficiency from the average. The bars are not indicators in the uncertainty in the estimation of the mean values of the simulations; they indicate the range of values expected when the stochastic process of phase variation has been used to determine the population transfer.

As one would expect, the presence of noise requires that pulse areas (parametrized by $\Omega_0\tau$) be increased to accomplish efficient population transfer. The need for larger pulse area can be anticipated from the fact that any two-photon detuning is detrimental to population transfer and that the two independent noise sources each contribute to this detuning.

Frames (a) and (b) of Fig. 3 differ in the magnitude of the noise fluctuations. In frame (b), with $D\tau=10$, the noise is sufficiently great that it prevents population transfer even for very large values of the pulse area. In frame (a), with $D\tau=2$, the noise effect, though appreciable, is much less severe.

Solid lines here, and in following figures, show the theoretical results of Sec. V, specifically Eqs. (5.3), (5.7), and (5.9). For the pulses of Eq. (3.16) the integral formulas simplify to Eqs. (5.8) and (5.10). The numerical and analytical results are obviously in excellent agreement for frame (a). The analytical result significantly underestimates the transfer efficiency in frame (b). This failure is to be expected from a perturbation theory that assumes high efficiency.

We have found good agreement between the analytical results and simulation for a wide range of noise parameter values such that the transfer efficiency is 0.5 or better. This agreement validates the use of the formulas to predict transfer efficiency for arbitrary combinations of γ and the noise parameters D and G.

For the limiting case of $T\to\infty$ considered here, we can predict the transfer efficiency for any pulses of finite duration. The prediction requires numerical evaluation of an integral, Eq. (5.9). Figure 4 shows the results of simulation with Gaussian pulses and of the theory based on numerical integration of Eq. (5.9).

B. Fully correlated fields ($T=0$)

Figure 5 presents further examples of simulation for pulses shape (3.16), this time for fully correlated fields ($T=0$). Again the Monte Carlo simulation (small circles) averaged 100 realizations of the stochastic process. Solid lines show the analytical results evaluated with expressions (5.3), (5.8), and (5.14). The agreement between simulation results and analytical results is excellent.

The noise-defining parameters are the same for Figs. 3 and 5. A comparison of frames (a) of the two figures shows that moderate fluctuations, which substantially affect the transfer efficiency for uncorrelated fields, have almost no

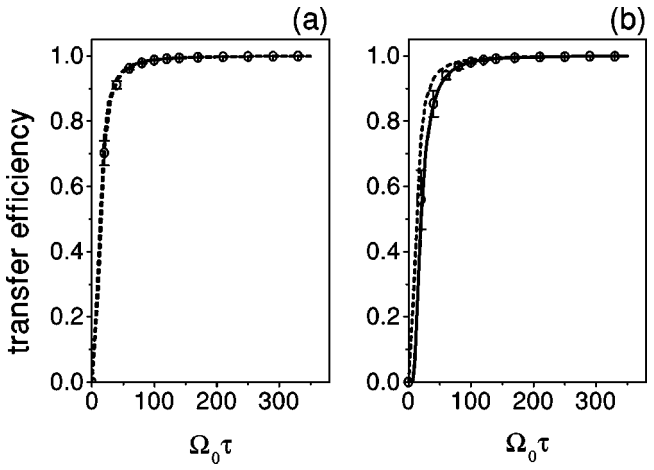

FIG. 5. Population transfer efficiency versus pulse area $\Omega_0\tau$, with $\delta=0$, $\Delta=0$, for pulses of shape (3.16). Fields have identical noise, $T=0$. Points and lines are as in Fig. 3. Parameters are $\gamma\tau=10$, $G\tau=50$. Frame (a) $D\tau=1$; frame (b) $D\tau=10$.

effect on the transfer efficiency when fluctuations becomes fully correlated. Conversely, if the noise noticeably hinders population transfer for correlated fields, then there will be very little transfer with uncorrelated fields.

When discussing Fig. 3(a) we noted that the detrimental effects of noise could be understood as variations in the two-photon detuning. In the present case, with $T=0$, the noise characteristic of the fields are identical, and so their contribution to the two-photon detuning cancels identically at all time. The consequences of noise are recognizable despite the fact that the two-photon detuning is zero at all times. This is because the one-photon detuning is affected by the noise. A rapidly varying phase hinders the adiabatic evolution and is thus detrimental to the population transfer. However the effect on the transfer efficiency is small.

We have also made simulations with the pulse shapes of Eq. (3.17). The results are very similar to those shown here; the small differences do not warrant a separate figure. Although we have no analytic expression from theory, there is an excellent fit between simulation and theoretical values obtained by numerical integration of Eq. (5.9).

C. Partially correlated fields

Figures 3 and 5, showing extreme cases of $T=0$ and $T=\infty$, displayed results whose qualitative properties could be anticipated: the presence of noise requires that pulse areas be increased to achieve the same high transfer efficiency that can be obtained without noise. As we demonstrate with Fig. 6, when the cross correlation of the two pulse phases does not have either of these extremes, unexpected results are evident. Figure 6 shows examples of simulations for partially correlated fields, plotting as before: the transfer efficiency versus pulse area (parametrized by the product of peak Rabi frequency Ω_0 and pulse duration τ). The set of frames displays results for different values of T. Frame (a), for which $T=2\tau$, can be regarded as a case of independently fluctuating fields. In the remaining frames T takes successively smaller values, and the fluctuations approach those of fully

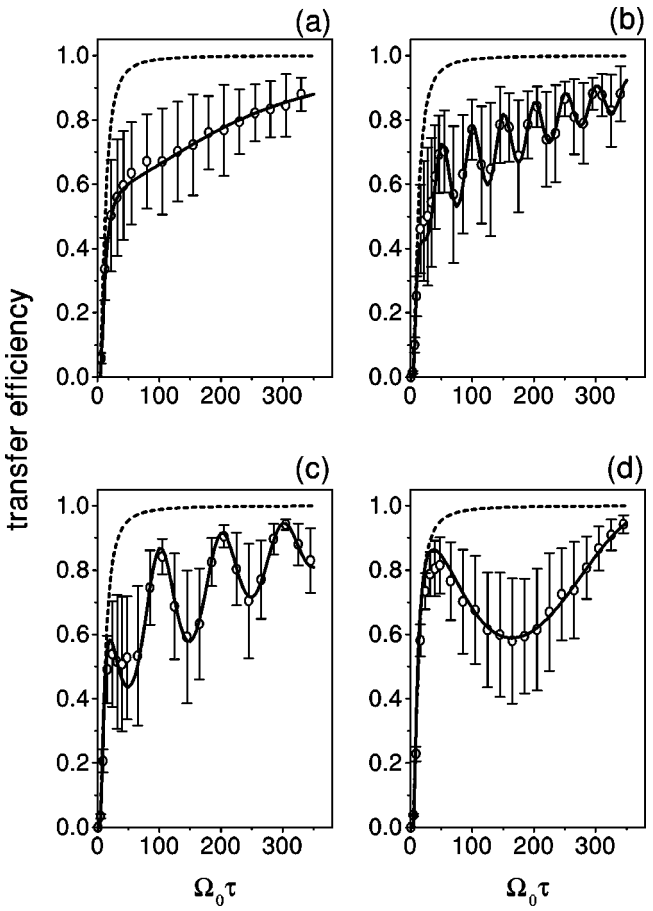

FIG. 6. Population transfer efficiency versus pulse area $\Omega_0\tau$, with $\delta=0$, $\Delta=0$, for pulses of shape (3.16) and various time delays T, with $\delta=0$, $\Delta=0$, $G\tau=100$, $\gamma\tau=10$, and $D\tau=1$. The display is as in Fig. 3. Parameters are (a) $T=2\tau$, (b) $T=\frac{1}{4}\tau$, (c) $T=\frac{1}{8}\tau$, and (d) $T=\frac{1}{32}\tau$.

correlated fields ($T=\frac{1}{4}\tau$, $T=\frac{1}{8}\tau$, $T=\frac{1}{32}\tau$), although T remains much longer than the correlation time $1/G$.

The simulation points, and the associated theoretical curves, exhibit striking and unexpected oscillations with increasing pulse area. These oscillations do not occur for the limiting cases of large T or for $T=0$, and they are not seen in frame (a), with $T=2\tau$. As T becomes smaller the frequency of these oscillations decreases, and their amplitude increases. This behavior is in excellent agreement with the theoretical results, Eqs. (5.3), (5.18), (5.19) depicted as solid lines. In the formulas the oscillations originate with a sine and cosine term whose argument is $(T/2)\sqrt{\Omega_0^2-\gamma^2/4}$. Thus when γ is small, variation of the area $\Omega_0\tau$ will produce oscillations with period $4\pi\tau/T$. The oscillations are predicted only for $T<\tau$. The theory predicts that for $\gamma\tau\gg1$ the oscillation amplitude is proportional to $\exp(-\gamma T/4)$. This function is small when T is comparable to or exceeds τ.

The theoretical work offers criteria for treating the fluctuations as independent. Obviously T must be large enough to permit damping all correlation between fields. The time delay must be also much longer than spontaneous emission time, $T\gg1/\gamma$, meaning that a fluctuation of one field will be forgotten by the atom by the time the fluctuation repeats in

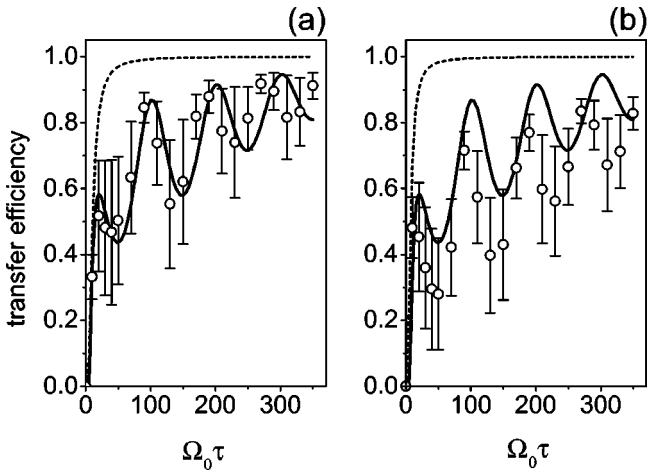

FIG. 7. Transfer efficiency versus $\Omega_0\tau$ for $T=(1/8)\tau$. Display and parameters are as in Fig. 6 (c). (a) For pulse shapes (3.17) with $t_d=0.6\tau$; (b) for Gaussian pulses (3.18) with $t_d=\tau$.

the other field. Finally, we require $T\gg 1/G$. This condition guarantees that the phases of the two fields are independent at any time. Both these last criteria must hold; if only $T\gg 1/G$ but $T\ll 1/\gamma$ then oscillations will occur. Both of these conditions are valid for the results shown in Fig. 3.

Although the analytic results apply rigorously only to pulses of the form (3.16), they can be used as a guide for predicting the effect of noise in other pulses. This is seen in Fig. 7(a), for the pulses of Eq. (3.17), and in Fig. 7(b) for Gaussian pulses. With both of these pulse shapes one sees the same qualitative behavior, of transfer efficiency that oscillates as a function of the pulse area; these features are not unique to the pulses (3.16) nor to pulses of finite duration.

The two pulse shapes give qualitatively similar results, although there are differences in quantitative details. In both frames the solid line repeats the theoretical curve for the pulse shape (3.16) depicted in Fig. 6, frame (c). We should expect that this theory would not give quantitative agreement with these simulations, but it does reproduce the qualitative features of the two examples.

We have found that the formula (5.18), though derived for the cos pulse shape (3.16), can be used to fit simulations for Gaussian pulses by introducing an ''effective'' constant value of Ω_{rms} instead of the time-dependent value that describes the Gaussian pulses, and by introducing an ''effective'' pulse duration. We have obtained these parameters by fitting the simulation results for $T\to\infty$ to the analytic form required for cos pulses, Eq. (3.16). When we used these in Eq. (5.18) for finite T, the agreement between the simulation and the theory was as good as can be obtained for the cos pulses.

V. ANALYTICAL RESULTS

It is well established that the crucial time interval for population transfer is while the Stokes pulse is decreasing and the pump pulse in increasing. For our analytic work we assume that at time $t=t_{begin}$ the Stokes pulse is at its maximum (with no pump field present) and all population resides in state ψ_1. We follow the time evolution only until the pump pulse reaches its maximum (and there is no longer any Stokes field). That is, we ignore the initial buildup of the Stokes pulse and the final dropping of the pump pulse, recognizing that in the absence of dual pulses the only effect of a single pulse is an unimportant phase increment of the initial and final states.

The presence of decay in Eq. (3.13) allows one to find solutions to the Schrödinger equation using perturbation theory. This was done for nonfluctuating fields in Ref. [25] for the two-photon resonant case $\delta=0$ and in Ref. [2] for $\delta\neq 0$. Phase noise can obviously be treated as dynamical two-photon and one-photon detunings, and the method developed in [2] for analyzing the two-photon line shape can be generalized to include the phase fluctuations. In this section we use perturbation theory to derive an approximate solution to the Schrödinger equation in the presence of (phase diffusion) noise for different cases of correlation between phase fluctuations. We compare this analytic solution with Monte Carlo simulation.

The analysis carried out here gives correct results for pulses such that, within a finite time interval, there occurs a large pulse area

$$\Omega_{rms}(t)\tau\gg 1, \quad t\in[t_{begin},t_{end}], \tag{5.1}$$

where t_{begin} and t_{end} are the initial and final moments of simultaneous interaction of the atom with both pulses. This condition ensures that, in the absence of phase fluctuations, the excitation will evolve adiabaticaly. We obtain a simple formula for the population transfer efficiency in the specific case of the pulse shape (3.16). Because a truly Gaussian pulse extends indefinitely in time, the criterion (5.1) is not strictly valid. However, for numerical simulation the time interval is finite and so the formula can be applied to these pulses as well.

Our perturbation treatment postulates that the amplitudes of Eq. (3.12) can be written as

$$C_d(t)=\exp[a_d(t)+b_d(t)],$$

$$C_b(t)=C_d(t)[a_b(t)+b_b(t)],$$

$$C_2(t)=C_d(t)[a_2(t)+b_2(t)], \tag{5.2}$$

where $b_j(t)$ are noise-dependent functions and $a_j(t)$ are functions independent of the noise. Then we write the expression for the transfer efficiency (the population of level 3 as $t\to\infty$) as the product of two factors

$$P=P^{(0)}\cdot P^{(\xi)}, \tag{5.3}$$

where $P^{(0)}$ describes the population transfer in the field of smooth pulses

$$P^{(0)}=\exp[2\ \mathrm{Re}\, a_d(\infty)] \tag{5.4}$$

and $P^{(\xi)}$, and ensemble average describes the noise-dependent part of the transfer efficiency

$$P^{(\xi)}=\langle\exp[2\ \mathrm{Re}\, b_d(\infty)]\rangle. \tag{5.5}$$

In an earlier work [2], perturbation theory was used to solve the Schrödinger equation for the case $\xi_P=\xi_S=0$ and $\delta\neq 0$. The small parameter in that work was $1/(\Omega_{max}\tau)$, where Ω_{max} is the maximum value of the rms Rabi frequency $\Omega_{rms}(t)$. It was also assumed that $\Omega_{max}\gg\gamma$. It was shown that the population transfer substantially decreases when $\delta\sim\Omega_{max}/\sqrt{\gamma\tau}$. This result implies that the noise will have an appreciable effect on the transfer efficiency only for two-photon detuning in the range of two-photon detning $\delta<\Omega_{max}/\sqrt{\gamma\tau}$.

In the present paper we develop the pertubation theory to apply beyond the range of [2], thereby allowing values of $\gamma\sim\Omega_{max}$. Such an extension is important for describing population transfer in atomic or molecular beams when the time of flight through the laser beams is significantly longer than the excited-state spontaneous emission lifetime.

We are concerned here primarily with situations in which the transfer efficiency is high. We will therefore approximate the average of an exponential $\langle\exp(x)\rangle$ by the exponential of an average $\exp(\langle x\rangle)$. Such an approximation is reliable as long as $\langle x^2\rangle\approx\langle x\rangle^2$. By doing so we express the noise-dependent part of the transfer efficiency as

$$P^{(\xi)}=\exp[2\,\mathrm{Re}\,\langle b_d(\infty)\rangle]. \tag{5.6}$$

The Appendix describes our approach to evaluating $b_d(t)$, from which the exponential argument is obtained by averaging over noise realizations.

A. The noise-free contribution $P^{(0)}$

Straightforward but cumbersome algebra (see the Appendix) gives the following result for the noise-free contribution to the transfer efficiency [see Eq. (5.3)]

$$P^{(0)}=\exp\left[-\int_{-\infty}^{+\infty}\left(4\gamma\frac{\dot\theta^2}{\Omega_{rms}^2}+\gamma\delta^2\frac{1-\cos 4\theta}{2\Omega_{rms}^2}+\delta^2\dot\Omega_{rms}\frac{1-\cos 4\theta}{\Omega_{rms}^5}(2\gamma^2-\Omega_{rms}^2)+2\delta^2\dot\theta\frac{\sin 4\theta}{\Omega_{rms}^4}(-\gamma^2+\Omega_{rms}^2)\right)dt\right]. \tag{5.7}$$

Here we have omitted the terms of order higher than δ^2 in the exponent. This expression can be evaluated numerically for any pulse shape that has finite time duration (pulses of infinite extent, such as Gaussians, may lead to diverging integrals). Note that the rms Rabi frequency Ω_{rms} appearing here will generally have some time dependence, though this is not shown explicitly.

For the pulse shape (3.16) the rms Rabi frequency is a constant $\Omega_{rms}=\Omega_0$ during the time interval when both pulses act. The integral (5.7) can then be evaluated analytically. The result is

$$P^{(0)}=\exp\left(-\frac{\gamma\pi^2}{\Omega_0^2\tau}-\frac{\delta^2\gamma\tau}{2\Omega_0^2}\right). \tag{5.8}$$

The first term describes nonadiabatic effects during the transfer [25] and the second term gives the two-photon line shape [2].

B. Uncorrelated fields (large $|T|$)

When the two laser fields fluctuate independently (as occurs when $|T|\to\infty$) the noise-dependent part of the transfer probability is expressible as [see the Appendix, Eq. (A15)]

$$P^{(\xi)}=\exp\left(-DG(2G+\gamma)\int_{-\infty}^{+\infty}\frac{1-\cos 4\theta(t)}{\Omega_{rms}(t)^2+4G^2+2\gamma G}dt\right). \tag{5.9}$$

This is the most general result of our theoretical work; it applies to arbitrary pulse shapes. As with the integral (5.7), this integral may diverge for pulses that extend over an infinite time. For pulses of finite duration, the integral can be evaluated numerically.

In obtaining expression (5.9) we made no assumption about pulse shape or sequence of interactions; the formula simply gives the noise-dependent part of the probability that the atom will remain in the dark state after the interaction with two laser pulses. It can be used together with Eqs. (5.3) and (5.7) to estimate the population of the dark state in the observation of dark resonances.

1. Special case: cos pulses

For the pulse shape (3.16) the integral in Eq. (5.9) can be evaluated analytically. The result is

$$P^{(\xi)}=\exp\left(-\frac{DG\tau(2G+\gamma)}{4G^2+2G\gamma+\Omega_0^2}\right). \tag{5.10}$$

Two limiting cases of this formula are of particular interest. When $G\to 0$ but the product $DG=N^2$ is fixed, we have an ensemble of pulses with constant carrier frequencies distribute around the average value. The second moment is N^2. In this limit the latter expression becomes

$$P^{(\xi)}=\exp\left(-\frac{N^2\gamma\tau}{\Omega_0^2}\right)\quad(G\to 0). \tag{5.11}$$

This coincides with what we obtain from Eq. (5.8) if we average the argument of the exponential over different two-photon detunings, taking into account $\langle\delta^2\rangle=2N^2$. In this case complete population transfer occurs when the bandwidth of each laser pulse is much less than the two photon linewidth $\Delta\omega=\sqrt{2}\Omega_0/\sqrt{\gamma\tau}$. A moderate increase of G to values $G\gtrsim\gamma$, while maintaining the condition $D<G$, has the same effect as narrowing the two-photon linewidth by increasing the decay rate of the excited state $\gamma\to\gamma+2G$.

Figure 8 illustrates the dependence of transfer efficiency upon noise characteristics by plotting contour lines showing the parameter combinations for which the transfer efficiency is 90%. The figure shows, in the same frame, both uncorrelated ($T\to\infty$) and fully correlated ($T\to 0$) noise. The axes

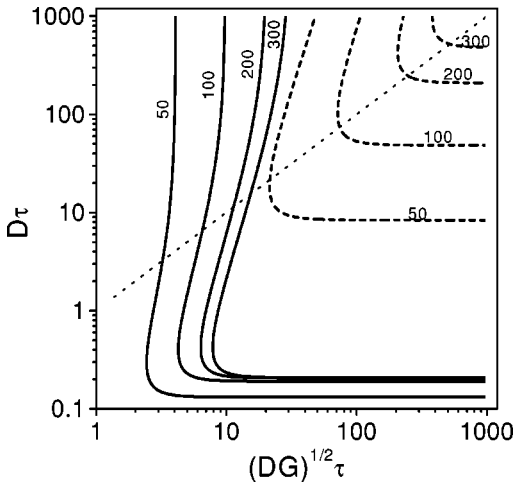

FIG. 8. Contours of 90% transfer efficiency. Solid lines, $T=\infty$; dashed lines, $T=0$. Curves are labeled with pulse area parameter $\Omega_0\tau$. The dotted line shows $G=D$. Parameters are $\gamma\tau=10$, $\delta=0$.

here differ deliberately from the earlier work of Kuhn *et al.* [17], who used D and G; our choice is based on the following observation.

For $D \ll G$ the noise spectrum has a Lorentzian shape, characterized by the width D. For $D \gg G$ the spectrum becomes Gaussian, with width $\sqrt{2\ln 2}\sqrt{DG}$. We have chosen these two widths as the scales for our axes, $y=D\tau$ and $x=\tau\sqrt{DG}$. The dashed line in each figure, marking $D=G$ separates the plot into two regions: far above this line the spectrum is Gaussian and the x axis gives the width; far below this line the spectrum is Lorentzian and the y axis gives the width. The asymptotes of the contours can be interpreted using the analytical formulas.

It should be noted that the usual Fourier limited bandwidth of a pulse refers to the spectrum of $A(t)\exp(i\phi)$, where $A(t)$ is the pulse amplitude and ϕ is the pulse phase. Here, when $G \gg D$, the parameter D is the half-width of the spectrum of $\exp(i\phi)$ alone. We see that here $D\tau \approx 0.2$. Therefore, the half-width D is just one-fifth of the Fourier limited bandwidth $1/\tau$.

For uncorrelated noise ($T\to\infty$) the lower (horizontal) asymptotes ($G \gg D$) move closer together as the pulse area increases. This limit is simply the noise-dependent part of the transfer efficiency because the noise-independent part gives unity. The vertical asymptotes [fixed DG, ($G\to 0$)] differ much more with pulse area; according to formula (5.11) they are proportional to the pulse area (if we neglect the noise-independent part of the transfer efficiency).

When the noise is fully correlated ($T=0$), the lower (horizontal) asymptotes depend substantially on the pulse area. (The apparent occurrence of a second asymptote in the region $D \gg G$ is a consequence of the logarithmic axes.) For fixed $y=D$ we have $G\to\infty$ when $x\to\infty$. In this region the noise is white noise. The other asymptote gives the case $G\to 0$, $D\to\infty$ with DG finite. In this region the effect of noise can be interpreted as the interaction of the atom with an ensemble of pulses with different two-photon detunings and constant phases.

2. A fundamental limit

An important limit of Eq. (5.10) occurs when $G\to\infty$ (white noise). In this case Eq. (5.10) reads

$$P^{(\xi)} = \exp(-\tfrac{1}{2}D\tau) \quad (G\to\infty). \tag{5.12}$$

Population transfer is small unless $D\tau \ll 1$. Here D represents the bandwidth of the laser. As shown in texts on laser theory, the basic (Schawlow-Townes) limit to the bandwidth of a laser is determined by spontaneous emission. It can be as small as a few Hz. This bandwidth imposes a fundamental limit on the transfer efficiency: when all ''technical'' noise has been eliminated, there remains a nonreducible bandwidth attributable to white noise. These uncontrollable fluctuations cannot be overcome by increasing Ω_0. By contrast, in the general case of a finite correlation time the transfer efficiency can be substantially increased by using more intense pulses, i.e., by increasing Ω_0 [see Eq. (5.10)]. As an example, for a linewidth of 1 Hz ($D=2\pi$ s^{-1}) and $\tau=10^{-5}$ s, the departure from complete population transfer is $1-P^{(\xi)} \approx 3\times 10^{-5}$.

C. Fully correlated fields ($T=0$)

When the two laser fields are generated by one source, and therefore have identical fluctuations (as occurs when $T=0$), the noise-dependent part of the transfer efficiency is given by the integral (see the Appendix)

$$P^{(\xi)} = \exp\left(-\int_{-\infty}^{+\infty} \frac{32DG^2\dot{\theta}(t)^2}{\Omega_{rms}(t)^2\tau[4G^2+2G\gamma+\Omega_{rms}(t)^2]}\,dt \right). \tag{5.13}$$

In general, for a given pulse shape, the integral must be evaluated numerically. However, for the pulse shape (3.16) the integral in Eq. (5.13) can be evaluated analytically, with the result

$$P^{(\xi)} = \exp\left(-\frac{8DG^2\pi^2}{\Omega_0^2\tau(4G^2+2G\gamma+\Omega_0^2)} \right). \tag{5.14}$$

For fixed product $DG=N^2$ and $G\to 0$ we obtain $P^{(\xi)}=1$. This is what one would expect from the fact that every realization of the noise maintains the two-photon resonance condition.

The case of finite but small $G \ll \Omega_0$ of Eq. (5.14),

$$P^{(\xi)} = \exp\left(-\frac{8N^2G\pi^2}{\Omega_0^4\tau} \right), \qquad G \ll \Omega_0 \tag{5.15}$$

gives a result differing from unity even though $\delta=0$. This can be interpreted as the effect departure from adiabatic evolution resulting from time-varying one-photon detuning .

A rough approximation to this situation is obtained by considering a frequency chirp, $\xi_P=\xi_S=\zeta t/\tau$, for the case $\Delta=0$ and $\delta=0$. This model gives a transfer efficiency of the form $P=P_0P_{chirp}$, where

$$P_{chirp}=\exp\left(-4\frac{\pi^2\zeta^2}{\Omega_0^4\tau^2}\right). \tag{5.16}$$

The analog of the variable ζ^2/τ, on which P_{chirp} depends, is N^2G in the case of fluctuating phases; both quantities are estimates of the rate of change of the square of the frequency (the time derivative of the phase). Taking into account this correspondence one can easily see that, within a numerical factor, the exponent of Eq. (5.15) looks like the exponent of Eq. (5.16). The numerical factor in Eq. (5.16) depends on the detailed time dependence of the phase derivatives $\xi_P=\xi_S$. They are different for a chirp and stochastic fluctuations. The qualitative agreement between Eqs. (5.15) and (5.16) confirms the interpretation of the effect of identical fluctuations on the efficiency of population transfer resulting from dynamical one-photon detuning.

The white noise limit ($G\to\infty$) of Eq. (5.14) gives the expression

$$P^{(\xi)}=\exp\left(-\frac{2D\pi^2}{\Omega_0^2\tau}\right), \quad G\to\infty. \tag{5.17}$$

In contrast to Eq. (5.12) there is no fundamental limit to the efficiency of the population transfer, which approaches unity arbitrarily closely for sufficiently large Ω_0. Comparison of Eqs. (5.17) and (5.8) reveals that white noise can substantially affect the efficiency of the population transfer if $2D \gg \gamma$. In the opposite case the efficiency of the population transfer is primarily determined by the noise-independent part of Eq. (5.3), as can be seen in Fig. 5(a).

D. Partially correlated fields (finite $|T|$)

In Sec. V C we analyzed the consequences on the transfer efficiency of identical fluctuations of the pump and Stokes fields ($T=0$). As is apparent from the simulations shown in Sec. IV C, partly cross-correlated fields have some unexpected consequences when used in a STIRAP process. The oscillatory variation of the transfer efficiency with increasing pulse area $\Omega_0\tau$ is a remarkable feature of our simulations.

As shown in the Appendix, we have derived analytic expressions for the transfer efficiency of partially cross-correlated fields in the special case when pulses have the shape (3.16). The degree of cross correlation is adjusted through the parameter T, which sets the delay between the noise fluctuations in the two fields. The result of the analysis is the formula [see the Appendix, Eq. (A15)]

$$P^{(\xi)}=\exp\left[-\frac{DG\tau}{4G^2+2G\gamma+\Omega_0^2}\left(2G+\gamma-\frac{\gamma\Omega_0^2e^{-G|T|}}{4G^2-2G\gamma+\Omega_0^2}\right)\right]\times\begin{cases}1, & |T|>\tau\\ \exp[g(T)], & |T|<\tau,\end{cases} \tag{5.18}$$

where

$$g(T)=\frac{2DG^2\exp\left(-\frac{1}{4}\gamma\left|T\right|\right)}{2\pi\Omega(4G^2+2G\gamma+\Omega_0^2)(4G^2-2G\gamma+\Omega_0^2)}\times\left[\pi(\tau-|T|)\cos\left(\frac{\pi T}{\tau}\right)+\tau\sin\left(\frac{\pi|T|}{\tau}\right)\right]\times\left[\gamma\sin\left(\frac{1}{2}\Omega\left|T\right|\right)(3\Omega_0^2+4G^2-\gamma^2)+2\Omega\cos\left(\frac{1}{2}\Omega T\right)(\Omega_0^2+4G^2-\gamma^2)\right], \tag{5.19}$$

and $\Omega=\sqrt{\Omega_0^2-\gamma^2/4}$. Alhough this formula is rather complicated, it is much easier to use than are simulations.

A careful consideration reveals that long-time correlation plays a crucial role in the dependence of the transfer efficiency upon the peak Rabi frequency. The Appendix presents details of the derivation of Eq. (5.18). There it is shown, in the first two equations of Eq. (A11), that for a class of pulse shapes the noise variables obey equations of an harmonic oscillator subject to a fluctuating driving force

$$F(t)=\frac{\Omega_{rms}}{4}[\xi_S(t)-\xi_P(t)]\sin 2\theta. \tag{5.20}$$

The response of this oscillator to the force is greatest when the force has large Fourier components near the resonant frequency of the oscillator, $\frac{1}{2}\Omega$. The response is weak to force frequencies that are far from resonance. If we assume that the resonant component of $\xi_P(t)$ is $A\exp(i/2\,\Omega t)$ then according to Eq. (3.21) the component of $\xi_S(t)$ is $A\exp[(i/2)\Omega(t+T)]$, and the difference of the components oscillates as $\exp(i/2\Omega T)$. If $\gamma T\ll 1$ then the near-resonant fluctuations destructively interfere—and the effects of noise are therefore least—when $\Omega T=4\pi n$ where n is any integer. When $\gamma T\gg 1$ the condition $\Omega T=4\pi n$ cannot hold for all fluctuation Fourier components inside the bandwidth of oscillator response, and therefore they do not interfere completely. For larger values of $|T|$ the interference becomes less pronounced. This explains the term $\exp(-\frac{1}{4}\gamma|T|)$ in expression (5.19). The most complete elimination of the noise influence obviously takes place for $T=0$.

Although we have treated the conventional lambda linkage pattern (see Fig. 1) which forms the basis for the usual STIRAP process, a similar analysis can be carried out for the ladder linkage pattern, in which the energy of level 3 lies above that of level 2. Whereas in the lambda pattern the two-photon detuning involves the difference between two carrier frequencies [see Eq. (3.8)], for a ladder pattern it is the sum of two frequencies. In that case the noise Fourier components interfere destructively—and noise effects are least—for time delay such that $\Omega T=2\pi(2n+1)$, where n is any integer. In this case the effect of noise is not small for $T=0$, as it is for the lambda linkage.

We see from Eqs. (5.11) and (5.12) that in different regimes different combinations of parameters are significant. For long autocorrelation times of the fluctuations, $G\to 0$, the

effect of the noise is determined by DG for uncorrelated noise but by DG^2 for fully correlated noise. In the limit $G \to \infty$ the effect of noise on the transfer efficiency is governed by the single parameter D.

VI. CONCLUSIONS

We have simulated the effect of phase noise on the population transfer efficiency of STIRAP processes, using the Ornstein-Uhlenbeck model of fluctuations. Our simulations include, by means of a time offset T, adjustable cross correlation of the pump and Stokes fields.

Using a perturbation theory, we have obtained analytic expressions for the transfer efficiency for a variety of pulse shapes in the limits $T=\infty$ and $T=0$. These agree well with the simulation results, for a wide range of noise parameters, except when the noise strongly inhibits population transfer.

In the limits $T=\infty$ and $T=0$ the transfer efficiency can always be improved by increasing the pulse areas. However, when the two fields are partially correlated, an increase in pulse area may actually be detrimental; the transfer efficiency exhibits remarkable and unexpected oscillatory dependence on pulse area. These oscillations are not unique to a particular choice of pulse shape, and appear to be a generic property of partially correlated fields. For a particular choice of pulse shape, Eq. (3.16), we have obtained analytic expressions for the transfer efficiency for partially cross-correlated fields. These results explain the oscillations quantitatively.

Our computer program is capable of simulating amplitude fluctuations as well as phase fluctuations, and we have examined a number of cases. As in the case of phase fluctuations, fully correlated noise ($T=0$) has much less effect on population transfer. We do not include such simulation results here because we have as yet no theory with which to compare them.

ACKNOWLEDGMENTS

L.P.Y. and V.I.R. acknowledge support by the DFG (436-UKR-113/46) and INTAS project 99-00019. We acknowledges financial assistance from a NATO collaborative research Grant No. 1507-826991.

APPENDIX: DERIVATION OF ANALYTICAL RESULTS

In this appendix we derive some useful expressions applicable to a wide variety of pulse shapes. The main requirement is that the pulses have finite temporal support—they must vanish outside some finite pulse duration. (In fact, our theoretical results are valid for infinitely long pulses if $\theta \to 0$ when $t \to -\infty$ and $\theta \to \pi/2$ when $t \to +\infty$ sufficiently quickly that the integral formula converges.)

The equations for the noise-independent functions a_b, a_2, a_d, derived by substituting the constructions of Eq. (5.2) into the RWA Schrödinger equation, are

$$\dot{a}_b + \dot{a}_d a_b = -\frac{i}{2}\delta a_b \cos 2\theta - \frac{i}{2}\Omega_{rms} a_2 + \dot{\theta} + \frac{i}{2}\delta \sin 2\theta,$$

$$\dot{a}_2 + \dot{a}_d a_2 = -\frac{i}{2}\Omega_{rms} a_b + \left(i\Delta - \frac{\gamma}{2}\right) a_2,$$

$$\dot{a}_d = -\dot{\theta} a_b + \frac{i}{2}\delta a_b \sin 2\theta + \frac{i}{2}\delta \cos 2\theta. \qquad \text{(A1)}$$

The corresponding equations for the noise-dependent functions b_b, b_2, and b_d are

$$\dot{b}_b + \dot{b}_d(b_b + a_b) = -\frac{i}{2}\Omega_{rms} b_2 - \dot{a}_d b_b - \frac{i}{2}\delta b_b \cos 2\theta - \frac{i}{2}\xi_P(1-\cos 2\theta)(a_b + b_b) - \frac{i}{2}\xi_S(1+\cos 2\theta)(a_b + b_b) + \frac{i}{2}(\xi_S - \xi_P)\sin 2\theta,$$

$$\dot{b}_2 + \dot{b}_d(b_2 + a_2) = -\frac{i}{2}\Omega_{rms} b_b - \dot{a}_d b_2 + \left(i\Delta - \frac{\gamma}{2}\right) b_2,$$

$$\dot{b}_d = -\dot{\theta} b_b + \frac{i}{2}\delta b_b \sin 2\theta - \frac{i}{2}\xi_P(a_b + b_b) \times \sin 2\theta + \frac{i}{2}\xi_S(a_b + b_b)\sin 2\theta - \frac{i}{2}\xi_P(1+\cos 2\theta) - \frac{i}{2}\xi_S(1-\cos 2\theta). \qquad \text{(A2)}$$

The following sections develop formulas for these quantities based on perterbation theory.

1. Population transfer in the fields of smooth pulses

Instead of the usual approach of introducing dimensionless quantities and small parameters based on them, we will formally treat $\Omega_{rms}\tau$ and $\gamma\tau$ as the terms of order $1/\epsilon^2$. Then the values of $\delta\tau$, $\xi_1\tau$, and $\xi_3\tau$ are of order $1/\epsilon$. Here we will not consider large one-photon detuning but will assume $\Delta\tau$ to be of the order of $1/\epsilon$. Inserting into the equations for a_b, a_2, a_d, where appropriate, the factors $1/\epsilon$ or $1/\epsilon^2$ to mark the order of magnitude of the corresponding values we get

$$\epsilon^2(\dot{a}_b + \dot{a}_d a_b) = -\frac{i}{2}\epsilon\delta a_b \cos 2\theta - \frac{i}{2}\Omega_{rms} a_2 + \dot{\theta}\epsilon^2 + \frac{i}{2}\epsilon\delta \sin 2\theta,$$

$$\epsilon^2(\dot{a}_2 + \dot{a}_d a_2) = -\frac{i}{2}\Omega_{rms} a_b + \left(i\epsilon\Delta - \frac{\gamma}{2}\right) a_2,$$

$$\epsilon\dot{a}_d = -\epsilon\dot{\theta} a_b + \frac{i}{2}\delta a_b \sin 2\theta + \frac{i}{2}\delta \cos 2\theta. \qquad \text{(A3)}$$

We stress here that ϵ is simply a symbol and should be changed to unity at the end of the evaluation. Taking into account that the characteristic time of variation of dark, bright, and excited states for smooth pulses is τ, one can see that the terms on the left-hand side of (A3) are small if γ and Ω_{rms} satisfy the conditions

$$\Omega_{rms}\tau \gg 1, \quad \gamma\tau \gg 1. \tag{A4}$$

We seek the solution of Eq. (A3) in the form

$$a_m = \sum_{n=-1}^{\infty} u_m^{(n)} \epsilon^n, \quad m = b,2,d. \tag{A5}$$

Substituting Eqs. (A5) in (A3) one can easily find a_b, a_2, and $\dot{a}_d$ with any desired precision. Following are the first four terms $u_n^{(d)}$. These give the value of $\dot{a}_d$ up to order ϵ^2.

$$\dot{u}_d^{(-1)} = \frac{i}{2}\delta \cos 2\theta,$$

$$\dot{u}_d^{(0)} = -\frac{1}{4}\frac{\delta^2 \gamma(1-\cos 4\theta)}{\Omega_{rms}^2},$$

$$\dot{u}_d^{(0)} = -i\frac{\delta^3(\cos 2\theta - \cos 6\theta)}{8\Omega_{rms}^2} + i\frac{\delta^2\Delta(1-\cos 4\theta)}{2\Omega_{rms}^2} + i\frac{\delta^3\gamma^2(\cos 2\theta - \cos 6\theta)}{4\Omega_{rms}^4},$$

$$\begin{aligned}\dot{u}_d^{(2)} = &-\frac{2\gamma\dot{\theta}^2}{\Omega_{rms}^2} - \frac{\delta^2\dot{\theta}\sin 4\theta}{\Omega_{rms}^2} + \frac{\delta^2\dot{\Omega}_{rms}(1-\cos 4\theta)}{2\Omega_{rms}^3} \\ &+ \frac{\delta^4\gamma(5\cos 8\theta - 4\cos 4\theta)}{16\Omega_{rms}^4} + \frac{\delta^3\Delta\gamma(\cos 2\theta - \cos 6\theta)}{\Omega_{rms}^4} \\ &+ \frac{\delta^2\gamma^2\dot{\theta}\sin 4\theta}{\Omega_{rms}^4} - \frac{\delta^4\gamma}{16\Omega_{rms}^4} - \frac{\delta^2\gamma^2\dot{\Omega}_0(1-\cos 4\theta)}{\Omega_{rms}^5} \\ &+ \frac{\delta^4\gamma^3(1+4\cos 4\theta - 5\cos 8\theta)}{16\Omega_{rms}^6}.\end{aligned} \tag{A6}$$

The fact that the series in ϵ for $\dot{a}_d$ starts from $1/\epsilon$ does not lead to any unphysical result. It simply gives the imaginary part of $a_d(\infty)$ and does not affect the probability of the population transfer. The zero-order part $u_d^{(0)}$ gives the two-photon line shape with good precision [2].

The terms in Eq. (A6), which do not contain time derivatives of Ω_{rms} or θ give the solution of Eq. (A3) in the adiabatic approximation. The decrease in population transfer due to this terms is caused by two-photon detuning, which mixes the decaying state ψ_2 into the adiabatic state of the Hamiltonian (3.6) that connects states ψ_1 and ψ_3 in the STIRAP process [2]. The other terms give the nonadiabatic correction. Substituting Eq. (A6) in Eq. (A5) and the result in Eq. (5.6) we get Eq. (5.7).

2. Population transfer in fluctuating fields

To derive the noise-dependent part of the transfer efficiency $P^{(\xi)}$, we have to take into account that the fields, and therefore the amplitudes of dark, bright and excited states, are not smooth functions of time in this case. We expect that the correlation time of fluctuations can be much smaller than the pulse duration. Imagine that all the a and b are small, and there are no fluctuations. Then with the neglect of the second-order terms the first two Eqs. (A2) become those of a damped harmonic oscillator. The solution will be damped oscillations with characteristic period Ω_{rms}. When there are rapid fluctuations, the oscillator will respond with the same characteristic time (for slow fluctuations the evolution will be adiabatic). Therefore, the quantities b_b and b_2 should vary with characteristic frequency Ω_{rms}, and we can expect $\dot{b}_b \sim \Omega_{rms} b_b$ and $\dot{b}_2 \sim \Omega_{rms} b_2$. [Generally Ω_{rms} is time dependent, but for the cos pulses of Eq. (3.16) it is constant.]

As in the preceding subsection we formally treat $\gamma\tau$ and $\Omega_{rms}\tau$ as being of order $1/\epsilon^2$ and treat $\delta\tau$, $\Delta\tau$, $\xi_1\tau$, and $\xi_3\tau$ as being of order $1/\epsilon$. Inserting the factors $1/\epsilon$ or $1/\epsilon^2$ into the Eqs. (A2) where appropriate, we obtain the equations

$$\begin{aligned}\dot{b}_b + \epsilon^2\dot{b}_d(b_b + a_b) = &-\frac{i}{2}\Omega_{rms}b_2 - \epsilon^2\dot{a}_d b_b - \frac{i}{2}\epsilon b_b\delta\cos 2\theta \\ &- \frac{i}{2}\epsilon(a_b + b_b)\xi_P(1-\cos 2\theta) \\ &- \frac{i}{2}\epsilon\xi_S(a_b + b_b)(1+\cos 2\theta) \\ &+ \frac{i}{2}\epsilon\sin 2\theta(\xi_S - \xi_P),\end{aligned}$$

$$\dot{b}_2 + \epsilon^2\dot{b}_d(b_2 + a_2) = -\frac{i}{2}\Omega_{rms}b_b - \epsilon^2\dot{a}_d b_2 + \left(i\epsilon\Delta - \frac{\gamma}{2}\right)b_2,$$

$$\begin{aligned}\epsilon\dot{b}_d = &-\epsilon\dot{\theta}b_d + \frac{i}{2}\epsilon\delta b_b\sin 2\theta \\ &- \frac{i}{2}\xi_P\sin 2\theta(a_b + b_b) \\ &+ \frac{i}{2}\xi_S\sin 2\theta(a_b + b_b) \\ &- \frac{i}{2}\xi_P(1+\cos 2\theta) \\ &- \frac{i}{2}\xi_S(1-\cos 2\theta).\end{aligned} \tag{A7}$$

We look for the solution of Eqs. (A7) as a perturbation series in the form

$$b_k = \sum_{n=-1}^{\infty} s_k^{(n)} \epsilon^n, \quad k=\{b,2,d\}. \tag{A8}$$

The following sections present expressions for the functions appearing here.

a. Zero order. No contribution to probability

The Eqs. (A7) in zero order in ϵ are

$$\dot{s}_b^{(0)} = -\frac{i}{2}\Omega_{rms} s_2^{(0)},$$

$$\dot{s}_2^{(0)} = -\frac{i}{2}\Omega_{rms} s_b^{(0)} - \frac{1}{2}\gamma s_2^{(0)},$$

$$\dot{s}_{-1}^{(d)} = -\frac{i}{2}\xi_P(1+\cos 2\theta) - \frac{i}{2}\xi_S(1-\cos 2\theta) + \frac{i}{2}(\xi_S - \xi_P + \delta) s_b^{(0)} \sin 2\theta. \tag{A9}$$

The solutions of these equations read

$$s_b^{(0)} = 0, \quad s_2^{(0)} = 0,$$

$$\dot{s}_d^{(-1)} = -\frac{i}{2}\xi_P(1+\cos 2\theta) - \frac{i}{2}\xi_S(1-\cos 2\theta). \tag{A10}$$

As in the case without fluctuations, the term $\dot{s}_d^{(-1)}$ is purely imaginary and therefore does not affect the probability of population transfer.

b. First order. A driven oscillator

From Eq. (A7) we derive the first-order equations

$$\dot{s}_b^{(1)} = -\frac{i}{2}\Omega_{rms} s_2^{(1)} + \frac{i}{2}\sin 2\theta[\xi_S - \xi_P],$$

$$\dot{s}_2^{(1)} = -\frac{i}{2}\Omega_{rms} s_b^{(1)} - \frac{1}{2}\gamma s_2^{(1)},$$

$$\dot{s}_d^{(0)} = -\frac{\gamma\delta}{4\Omega_{rms}^2}(\xi_S - \xi_P)(1-\cos 4\theta) + \frac{i}{2}(\xi_S - \xi_P + \delta) s_b^{(1)} \sin 2\theta. \tag{A11}$$

The first two Eqs. of Eq. (A11) describe a damped harmonic oscillator with unit mass and time-dependent eigenfrequency $\frac{1}{2}\Omega_{rms}$ driven by the stochastic force

$$F(t) = \frac{\Omega_{rms}}{4}\sin 2\theta[\xi_S(t) - \xi_P(t)]. \tag{A12}$$

This equation can be solved for arbitrary ξ_P, ξ_S. The result is

$$s_b^{(1)}(t) = \int_{-\infty}^{t} dt' \frac{\Omega_{rms}(t')\sin 2\theta(t')}{2\Omega(t')\Omega_{rms}(t)}[(\xi_P(t') - \xi_S(t')] \times [\lambda^*(t)F(t,t') - \lambda(t)F^*(t,t')], \tag{A13}$$

$$s_2^{(1)}(t) = \int_{-\infty}^{t} dt' \frac{i\Omega_{rms}(t')\sin 2\theta(t')}{4\Omega(t')}[\xi_P(t') - \xi_S(t')] \times [F(t,t') - F^*(t,t')], \tag{A14}$$

where $\Omega(t) = \sqrt{\Omega_{rms}(t)^2 - \frac{1}{4}\gamma^2}$, $\lambda(t) = -\frac{1}{4}\gamma + \frac{i}{2}\Omega(t)$, and $F(t,t') = \exp(\int_{t'}^{t}\lambda(t'')dt'')$. Substituting Eq. (A14) into the third equation of Eq. (A11) we find $\dot{s}_d^{(0)}$. We integrate this to obtain $s_d^{(0)}$, which we average to obtain the noise-dependent part of the transfer efficiency [having made the approximation leading from Eq. (5.5) to Eq. (5.6)]

$$P^{(\xi)} \approx \exp\left[2\ \mathrm{Re}\int_{-\infty}^{\infty}\langle \dot{s}_d^{(0)}(t)\rangle dt\right] = \exp\langle 2\ \mathrm{Re}\, s_d^{(0)}(\infty)\rangle. \tag{A15}$$

To evaluate the stochastic averabe $\langle s_d^{(0)}(t)\rangle$ we use Eq. (2.2) and neglect $\exp(-\frac{1}{4}\gamma\tau)$ compared with unity. For the case $|T| > \tau$ and $G|T| \gg 1$ (independent fluctuations of different pulses) we obtain Eq. (5.9). Correlation between fluctuations of different pulses leads to more complicated expression for the transfer efficiency. For the pulse shape (3.16) we obtain Eq. (5.18).

c. Higher order

When Eq. (5.19) is taken into account the expression (5.18) for P with $T=0$ is identically equal to unity. Therefore it does not describe the effect of any fluctuations. To obtain a description of fluctuations when $T=0$ one must deal with higher-order terms in Eq. (A8). The procedure is the same as in the earlier case. We assume $\xi_P = \xi_S$ and solve a chain of equations. The b_d term of order $d=-1$ is a purely imaginary number; it gives a fluctuating phase. The terms of order 0, 1, and 2 all vanish identically. The term of order 3 is nonzero, but it vanishes after averaging over an ensemble. The lowest-order nonzero real-valued contribution to the average $\langle \dot{b}_d\rangle$ comes from the fourth-order term $s_d^{(4)}$; it gives Eq. (5.14).

[1] K. Bergmann, H. Theuer, and B. W. Shore, Rev. Mod. Phys. **70**, 1003 (1998).
[2] V. I. Romanenko and L. P. Yatsenko, Opt. Commun. **140**, 231 (1997).
[3] J. H. Eberly, K. Wodkiewicz, and B. W. Shore, Phys. Rev. A **30**, 2381 (1984).
[4] K. Wodkiewicz, B. W. Shore, and J. H. Eberly, Phys. Rev. A **30**, 2390 (1984).
[5] R. M. Whitley and C. R. Stroud, Jr., Phys. Rev. A **14**, 1498 (1976).
[6] F. T. Hioe and J. H. Eberly, Phys. Rev. Lett. **47**, 838 (1981).
[7] E. Arimondo, Prog. Opt. **35**, 259 (1996).
[8] B. J. Dalton and P. L. Knight, J. Phys. B **15**, 3997 (1982).
[9] B. Dalton and P. L. Knight, Opt. Commun. **42**, 411 (1982).
[10] R. J. Glauber, in *Quantum Optics and Electronics*, edited by C. DeWitt, A. Blandin, and C. Cohen-Tannoudji (Gordon and Breach, New York, 1965).
[11] N. G. Van Kampen, *Stochastic Processes in Physics and Chemistry* (North-Holland, New York, 1981).
[12] J. H. Eberly, Phys. Rev. Lett. **37**, 1387 (1976).
[13] J. L. F. de Meijere and J. H. Eberly, Phys. Rev. A **17**, 1416 (1978).
[14] G. S. Agarwal, Phys. Rev. A **18**, 1490 (1978).
[15] A. T. Georges and P. Lambropoulos, Phys. Rev. A **18**, 587 (1978).
[16] A. T. Georges, Phys. Rev. A **21**, 2034 (1980).
[17] A. Kuhn, S. Schiemann, G. Z. He, G. Coulston, W. S. Warren, and K. Bergmann, J. Chem. Phys. **96**, 4215 (1992).
[18] S. N. Dixit, P. Zoller, and P. Lambropoulos, Phys. Rev. A **21**, 1289 (1980).
[19] M. H. Anderson, R. D. Jones, J. Cooper, S. J. Smith, D. S. Elliott, H. Ritsch, and P. Zoller, Phys. Rev. Lett. **64**, 1346 (1990).
[20] M. H. Anderson, R. D. Jones, J. Cooper, S. J. Smith, D. S. Elliott, H. Ritsch, and P. Zoller, Phys. Rev. A **42**, 6690 (1990).
[21] K. Wodkiewicz, B. W. Shore, and J. H. Eberly, J. Opt. Soc. Am. B **1**, 398 (1984).
[22] R. F. Fox, I. R. Gatland, R. Roy, and G. Vemuri, Phys. Rev. A **38**, 5938 (1988).
[23] G. Vemuri and R. Roy, Opt. Commun. **77**, 318 (1990).
[24] B. W. Shore, *The Theory of Coherent Atomic Excitation* (Wiley, New York, 1990).
[25] M. Fleischhauer and A. S. Manka, Phys. Rev. A **54**, 794 (1996).